Oxygen reaction-diffusion in metalorganic chemical vapor deposition HfO 2 films annealed in O 2

K. P. Bastos, J. Morais, L. Miotti, R. P. Pezzi, G. V. Soares, I. J. R. Baumvol, R. I. Hegde, H. H. Tseng, and P. J. Tobin

Citation: Applied Physics Letters **81**, 1669 (2002); doi: 10.1063/1.1502006
View online: http://dx.doi.org/10.1063/1.1502006
View Table of Contents: http://scitation.aip.org/content/aip/journal/apl/81/9?ver=pdfcov
Published by the AIP Publishing

Oxygen reaction-diffusion in metalorganic chemical vapor deposition HfO_2 films annealed in O_2

K. P. Bastos, J. Morais,[a] L. Miotti, R. P. Pezzi, G. V. Soares, and I. J. R. Baumvol
Instituto de Física, Universidade Federal do Rio Grande do Sul, Av. Bento Gonçalves, 9500-91509-900 Porto Alegre, Brazil

R. I. Hegde, H. H. Tseng, and P. J. Tobin
Advanced Process Development and External Research, Digital DNA Laboratories, Motorola, Austin, Texas 78721

(Received 6 May 2002; accepted for publication 2 July 2002)

Composition, atomic transport, and chemical reaction were investigated following annealing in O_2 of ultrathin HfO_2 films deposited on Si substrates thermally nitrided in NO. The as-prepared thin film composition was established by Rutherford backscattering spectrometry, nuclear reaction analysis, and x-ray photoelectron spectroscopy as a HfO_2 film on an intermediate layer containing silicon oxynitride, hafnium silicate, and possibly hafnium–silicon oxynitride. O penetration, incorporation in the bulk of the HfO_2/SiO_xN_y structure, and oxidation of the substrate forming SiO_2 were observed. © *2002 American Institute of Physics.* [DOI: 10.1063/1.1502006]

Among the potential candidates for replacement of SiO_2 or SiO_xN_y as gate dielectric[1] hafnium oxide (HfO_2) seems to be one of the most promising materials,[2–5] combining high dielectric permittivity with low leakage current due to a reasonably high barrier height that limits electron tunneling.[6] Other requirements[7,8] on gate dielectric materials like low density of interface states, gate compatibility, structural, physical, and chemical stability at both gate electrode/dielectric and dielectric/Si interfaces are currently making the object of intensive investigation as semiconductor manufacturers are anticipating sub-0.1 μm channel length devices using high-k dielectrics, most probably hafnium oxides and/or silicates.

Previous studies[1] in other high-k ultrathin films on Si indicated that the interface layer thickness and composition can vary according to the deposition method and routine, and various species can be transported during post deposition thermal processing, like oxygen,[9,10] Si,[11–13] and the metal species,[14,15] altering the atomic concentrations as well as chemical composition of the system and consequently electrical characteristics like dielectric constant, interface density of states, and mobility of charge carriers in the transistor channel. In particular, stability against annealing in O_2-containing atmospheres is of high interest, since in further processing steps it is either performed intentionally to improve leakage current and CET characteristics[1,7,8] or unintentionally, because oxygen is almost always residual in any production furnace.

We report here on atomic composition and transport and on chemical reaction studies during annealing in oxygen of 5.0 nm (ellipsometric determination) polycrystalline HfO_2 films deposited on Si(001) substrates which were thermally oxynitrided in NO prior to metal oxide deposition. The starting structure was prepared by following sequence: HF cleaning of silicon wafers, followed by annealing in NO, and followed by metalorganic chemical vapor deposition (MOCVD) of HfO_2 at 550 °C using Hf-t-butoxide. The wafers were then submitted to postdeposition rapid thermal annealing (RTA) in Ar:N_2 at 1000 °C for 10 s (Ar annealing), in order to simulate a typical dopant-annealing step. Finally, the wafers were submitted to RTA in O_2 at 800 °C for 10 or 60 s (O_2 annealing), simulating any of the several usual thermal processing steps, including those intentionally performed in O_2. This last annealing step was also alternatively performed in 7×10^3 Pa of O_2 97%-enriched in the ^{18}O isotope ($^{18}O_2$ annealing), allowing to distinguish between oxygen incorporated from the gas phase and that previously existing in the as-prepared films. Furthermore, these $^{18}O_2$ annealings were performed with and without Ar preannealing, aiming at investigating the effects of the two thermal steps separately. The areal densities and concentration versus depth distributions of the different atomic species were determined by Rutherford backscattering of He^+ ions in a channeling geometry with grazing angle detection of the scattered ions [channeled Rutherford backscattering spectroscopy-(RBS)],[16] by nuclear reaction analysis (NRA),[16] and by narrow nuclear resonant reaction profiling (NRP)[16] of O and Si. Chemical composition and reaction were accessed by x-ray photoelectron spectroscopy using a Mg $K\alpha$ x-ray source and an emission angle between the sample normal and the axis of the electron energy analyzer of 25°.

Figure 1(a) shows the Si, O, and N signals in channeled-RBS spectra of 1 MeV incident He^+ ions from as-prepared and O_2-annealed samples, with the Hf signals in the inset. The areal densities of Hf and Si (as determined by channeled-RBS) and of ^{16}O and ^{14}N (as determined by NRA) are given in Table I. O_2 annealing for 60 s (sample 3 in Table I) produces an increase on the O-areal density of about 30% with respect to the as-prepared sample (sample 1) and a comparable percentage decrease on the N-areal density. Figure 1(b) shows Si, ^{16}O, and ^{18}O signals in channeled-RBS spectra of $^{18}O_2$-annealed samples for 10 s, with and without Ar

[a]Electronic mail: jonder@if.ufrgs.br

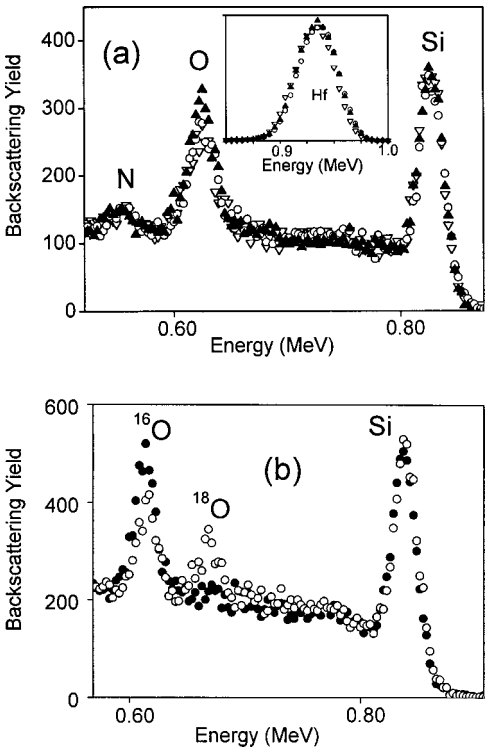

FIG. 1. (100) Channeled-RBS spectra of 1 MeV incident He^+, with detection of the scattered ions at 100° with the direction of incidence: (a) as-prepared sample (open down triangles), Ar annealing at 1000 °C for 10 s followed by O_2 annealing at 800 °C for 10 s (open dots) and 60 s (solid triangles). The corresponding Hf signals are shown in the inset; (b) Ar annealing at 1000 °C for 10 s followed by $^{18}O_2$ annealing at 800 °C for 10 s (solid dots) and $^{18}O_2$ annealing only at 800 °C for 10 s (open dots).

preannealing (samples 5 and 6 in Table I). One notices the presence of $^{16}O-^{18}O$ exchange, which increases with time of annealing in $^{18}O_2$ and is much larger for samples that were annealed in $^{18}O_2$ only then for those that were preannealed in Ar. $N-^{18}O$ exchange probably also occurs[16] as a parallel process to $^{16}O-^{18}O$ exchange.

Excitation curves of the $^{18}O(p,\alpha)^{15}N$ nuclear reaction

TABLE I. Areal densities (in units of 10^{15} cm^{-2}) of different atomic species and isotopes. Ar annealing at 1000 °C, O_2, and $^{18}O_2$ annealing at 800 °C. Errors in the areal densities are 10% for Si, and ^{14}N, 5% for Hf and ^{16}O, and 3% for ^{18}O.

	Hf	Si	^{16}O	^{18}O	^{14}N
(1) As-prepared	9.5	1.4	22.2	0.02	1.6
(2) Ar anneal+ O_2 anneal 10 s	9.6	1.4	24.3	0.02	1.5
(3) Ar anneal+ O_2 anneal 60 s	9.8	1.8	28.5	0.02	1.2
(4) Ar anneal	9.6	1.5	23.2	0.02	1.6
(5) Ar anneal+ $^{18}O_2$ anneal 10 s	9.6	1.5	22.4	0.51	1.5
(6) $^{18}O_2$ anneal 10 s	9.8	1.7	19.1	6.54	1.4
(7) Ar anneal+ $^{18}O_2$ anneal 60 s	9.5	1.7	22.3	4.76	1.2
(8) $^{18}O_2$ anneal 60 s	9.6	2.2	15.4	11.13	1.1

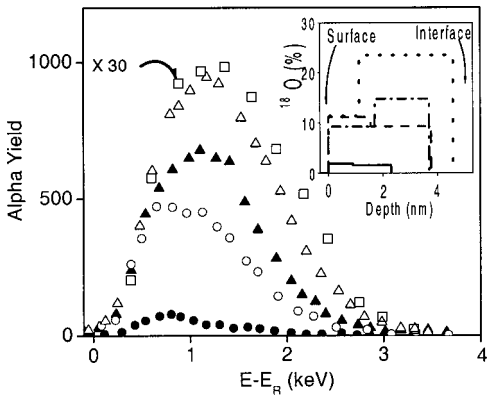

FIG. 2. Excitation curves of the $^{18}O(p,\alpha)^{15}N$ nuclear reaction around the resonance at 151 keV with the corresponding ^{18}O profiles in the inset: as-prepared sample (open squares, ×30), Ar annealing at 1000 °C for 10 s followed by $^{18}O_2$ annealing at 800 °C for 10 s (solid dots, solid curve) and 60 s (solid triangles, dash-dot curve), and $^{18}O_2$ annealing only at 800 °C for 10 s (open dots, dash curve) and 60 s (open triangles, dot curve).

around the resonance at 151 keV ($\Gamma_R = 100$ eV) and ^{18}O profiles (depth resolution of approximately 0.7 nm near the surface)[16] of as-prepared and $^{18}O_2$-annealed samples are shown in Fig. 2. The ^{18}O profiles in samples 5 and 7 (preannealing in Ar+10 or 60 s $^{18}O_2$ annealing) indicate a propagating ^{18}O front from the surface and reaction (eventually $^{16}O-^{18}O$ and $N-^{18}O$ exchange reactions only) with the HfO_2 network. Furthermore, ^{18}O profiles in samples 6 and 8 ($^{18}O_2$ annealing only for 10 and 60 s) are deeper and higher. When compared to similar studies performed previously[9–13] in aluminum, zirconium, and gadolinium oxides and silicates, the present HfO_2/SiO_xN_y structure displays higher resistance to oxygen migration from the gas into the solid phase and incorporation therein, as well as smaller isotopic exchanges. ^{29}Si profiles were determined by NRP[16] (results not shown here), revealing that Si remains immobile during annealing, in contrast to several of the earlier mentioned materials where substrate Si is seen to migrate into the oxide film.[9,11–13]

Figure 3 shows Si $2p$ photoelectron regions for as-prepared and O_2-annealed (10 and 60 s) samples. The Hf $4f$ and O $1s$ regions for the as-prepared sample are shown in the insets, being almost identical to those for the annealed samples. The Si $2p$ region for the starting sample has three components, one around the binding energy of 99.5 eV commonly associated with Si–Si bond (Si–Si component), another around 103.2 eV associated with different Si–O bonding configurations, including Si–O–Hf bond (Si–O component),[17,18] and a third, much smaller component around 101 eV associated with Si in an oxynitride bonding configuration (Si–O–N component).[18] According to literature[8,17,18] the Hf $4f$ signal here observed is mostly due to HfO_2, although minor contributions from Hf–O–Si and Hf–O–N bonds cannot be excluded. Similarly, the O $1s$ signal is attributed[17] mainly to O–Hf bond. The film composition is then essentially HfO_2, whereas the interface region has a complex composition, including SiO_2, SiO_xN_y, $Si_xHf_xO_z$[3] and $Si_kHf_xO_yN_z$. The Si–Si/Si–O area ratio increases significantly from the as-prepared to the 10 s O_2-annealed sample, which could be indicative either of chemical reactions taking place at the interface, like hafnium

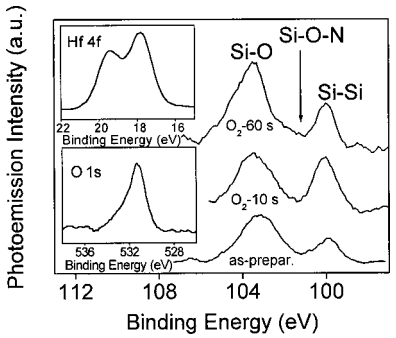

FIG. 3. Si $2p$ photoelectron regions for the as-prepared sample and Ar annealed at 1000 °C for 10 s followed by O_2 annealing at 800 °C for 10 and 60 s. The Hf $4f$ and O $1s$ regions for the as-prepared sample are shown in the insets.

silicide formation by oxides reduction or of higher Si–Si contribution due to loss of atoms from the HfO_2/SiO_xN_y film. However, this ratio remains constant from the as-deposited to the 60 s O_2-annealed sample, excluding these possibilities. RBS and NRA data of Table I also exclude HfO_2/SiO_xN_y losses as a possibility. Owing to substantial thinning of the HfO_2 films[3,5] following Ar annealing, an increase of the Si–Si component contribution from the substrate is expected. The subsequent O_2 annealing for 10 s does not lead significant oxygen from the gas phase to oxidize Si at the interface (see Figs. 1 and 2 and Table I). Consequently, an increase in the Si–Si/Si–O ratio is observed. On the other hand, a subsequent 60 s O_2 annealing increases substantially the oxygen content, as well as it leads oxygen from the gas phase to reach the interface, oxidizing substrate Si and thus compensating the increase of the Si–Si component from the substrate due to thinning by a comparable increase of the Si–O component.

Figure 4 shows typical Hf-signal regions in RBS spectra from samples whose oxide and oxynitride layers were tentatively removed by means of concentrated HF etching.[14,15] Indeed, the absence of O signal in the inset indicates that, within the sensitivity of RBS, the removal process was effective. Thus, unless for a possible incomplete etching of the oxide and oxynitride layers, thermally activated Hf migration into Si seems to occur, consistent with previous observation in Zr and Hf silicate films on Si.[14,15] A Hf profile could be inferred in the Ar-annealed sample by tilting in a special geometry,[13] which gives a depth resolution of approximately 2 nm. These RBS analyses indicate that Hf would penetrate into Si to areal densities of the order of 10^{12} cm^{-2} and a maximum range of approximately 4 nm.

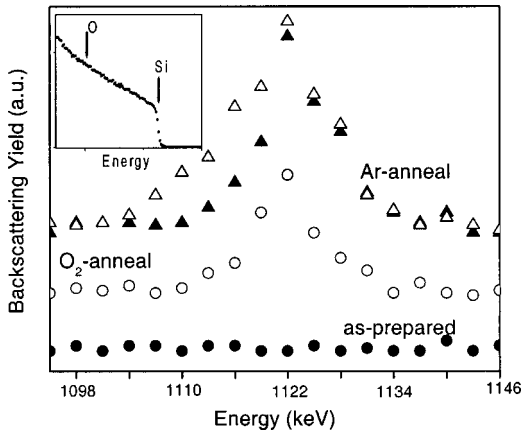

FIG. 4. Hf signal in RBS spectra of 1.2 MeV incident He^+ ions of samples after oxide and oxynitride layers removal by HF-etching: as-prepared sample (solid dots), $^{18}O_2$ annealed only at 800 °C for 60 s (open dots), and Ar annealed only at 1000 °C for 10 s measured at normal incidence (solid triangles) and 85° tilt (open triangles). The O and Si signals for the Ar-annealed sample are shown in the inset.

In summary, the present characterizations indicate that this structure is essentially stable against Ar preannealing at 1000 °C and O_2 annealing at 800 °C. For the annealing temperatures and times of the present work, the HfO_2/SiO_xN_y structure showed to be more resistant to O and Si migration and incorporation than others studied previously, with the Ar preannealed samples exhibiting a higher resistance than those directly annealed in O_2. We attribute this stability to a synergism between the properties of HfO_2 films on Si and the reaction-diffusion barrier constituted by both the SiO_xN_y interlayer and N eventually incorporated into the HfO_2 films.

The authors thank Joe Mogab, Betsy Weitzman, and Steve Anderson for the management support. The authors also thank Ricardo Garcia, and APRDL Process Engineering for their assistance with the metal oxide depositions. Financial support from CNPq and FAPERGS (Brazil) is acknowledged.

[1] G. D. Wilk, R. M. Wallace, and J. M. Anthony, J. Appl. Phys. **89**, 5243 (2001).
[2] B. K. Park, J. Park, M. Cho, C. S. Hwang, K. Oh, Y. Han, and D. Y. Yang, Appl. Phys. Lett. **80**, 2368 (2002).
[3] S. Sayan, S. Aravamudhan, B. W. Busch, W. H. Schulte, F. Cosandey, G. D. Wilk, T. Gustafsson, and E. Garfunkel, J. Vac. Sci. Technol. A **20**, 507 (2002).
[4] S. A. Campbell, T. Z. Ma, R. Smith, W. L. Gladfelter, and F. Chen, Microelectron. Eng. **59**, 361 (2001).
[5] K.-J. Choi, W.-C. Shin, and S.-G. Yoon, J. Electrochem. Soc. **149**, F18 (2002).
[6] S. Sayan, E. Garfunkel, and S. Suzer, Appl. Phys. Lett. **80**, 2135 (2002).
[7] A. I. Kingon, J. P. Maria, and S. K. Streiffer, Nature (London) **406**, 1032 (2000).
[8] B. H. Lee, L. Kang, R. Nieh, W.-J Qi, and J. C. Lee, Appl. Phys. Lett. **76**, 1926 (2000).
[9] B. W. Busch, W. H. Schulte, E. Garfunkel, T. Gustafsson, W. Qi, R. Nieh, and J. Lee, Phys. Rev. B **62**, 13290 (2000).
[10] D. Landheer, X. Wu, J. Morais, I. J. R. Baumvol, R. P. Pezzi, L. Miotti, W. N. Lennard, and J. K. Kim, Appl. Phys. Lett. **79**, 2618 (2001).
[11] M. Kundu, N. Miyata, and M. Ichikawa, Appl. Phys. Lett. **78**, 1517 (2001).
[12] C. Krug, E. B. O. da Rosa, R. C. M. de Almeida, J. Morais, I. J. R. Baumvol, T. D. M. Salgado, and F. C. Stedile, Phys. Rev. Lett. **86**, 4714 (2001); M. Copel, *ibid.* **86**, 4713 (2001).
[13] J. Morais, E. B. O. da Rosa, L. Miotti, R. P. Pezzi, I. J. R. Baumvol, A. L. P. Rotondaro, M. J. Bevan, and L. Colombo, Appl. Phys. Lett. **78**, 2446 (2001).
[14] M. Quevedo-Lopez, M. El-Bouanani, S. Addepalli, J. L. Duggan, B. E. Gnade, M. R. Visokay, M. Douglas, M. J. Bevan, and L. Colombo, Appl. Phys. Lett. **79**, 2958 (2001).
[15] M. Quevedo-Lopez, M. El-Bouanani, S. Addepalli, J. L. Duggan, B. E. Gnade, M. R. Visokay, M. Douglas, and L. Colombo, Appl. Phys. Lett. **79**, 4192 (2001).
[16] I. J. R. Baumvol, Surf. Sci. Rep. **36**, 1 (1999), and references therein.
[17] G. D. Wilk, R. M. Wallace, and J. M. Anthony, J. Appl. Phys. **87**, 484 (2001).
[18] M. R. Visokay, J. J. Chambers, A. L. P. Rotondaro, A. Shanware, and L. Colombo, Appl. Phys. Lett. **80**, 3183 (2002).